References

[1] Cox, A. L., "Report on the analysis of the available information on electrification produced by the dynamic interaction of liquids with solids," Final Report on Contract DA-19-020-ORD-5452 (February 6, 1962).

[2] Smith, J. M., "Theoretical study of the electrohydrodynamic generator," General Electric Rept. R61SD192, AF33(616)-7539 (November 1961).

[3] Marks, A. M., "Heat-electrical power conversion through the medium of a charged aerosol," U. S. Patent 2,638,555 (May 12, 1953).

[4] Smith, W. P., "Electrostatic voltage power generator," U. S. Patent 2,643,349 (June 23, 1953).

[5] Cox, A. L., et al., "Reports on propellants for electrical propulsion engines of the contact or bombardment ion type," Rocketdyne R-2513-1, 2, and 3, AF33(616)-7063 (July 1960, October 1960, and January 1961).

[6] Lewis, B., Pease, R. N., and Taylor, H. S. (eds.), "Combustion processes," *High Speed Aerodynamics and Jet Propulsion* (Princeton University Press, Princeton, N. J., 1956), Vol. II, pp. 52–62.

[7] Courtney, W. G., "Kinetics of condensation from the vapor phase," Texaco Experiment Inc. TM-1340, NOnr-3141(00) (July 15, 1962).

[8] Hamilton, R. C., "Interplanetary space probe auxiliary power systems," ARS Preprint 864-59 (June 1959).

[9] Molitor, J. H., et al., "Final report, analytical studies on ion propulsion," Rocketdyne R-2495P, ARL-TR-60-320 (June 1960).

NOVEMBER 1963 AIAA JOURNAL VOL. 1, NO. 11

Plasma Behavior in an Oscillating-Electron Ion Engine

J. W. Davis,* A. W. Angelbeck,† and E. A. Pinsley‡

United Aircraft Corporation, East Hartford, Conn.

The behavior of the plasma within an oscillating-electron ion engine was investigated in detail. It was found that certain conditions of gas pressure, magnetic field strength, and cathode emission current are required to maintain the accelerating electrostatic field in the plasma within the engine. In addition, the investigation revealed two types of transient phenomena in the discharge which can occur under certain conditions. The first is a pulsing or fluctuating mode of operation which appears to be caused by depletion of gas within the engine due to the pumping action of the discharge. The second is an azimuthal rotation of plasma perturbations in the range of frequencies of 10 to 50 kc as a result of $E_r \times B_x/B^2$ drifts. There is a possibility that this rotation may result in an enhanced diffusion of electrons across the containing magnetic field and hence contribute to engine power losses.

Nomenclature

B = magnetic flux density
D = diffusion coefficient
E = electric field
I = current
M = molecular weight
$\dot{m}$ = mass flow
P_c = probability of collision
p = pressure
T = temperature
V_{pE} = exhaust beam plasma potential
ω = cyclotron frequency
τ = mean free time

Subscripts

a = anode
i = ion
r = radial direction
s = solenoid
x = axial direction
θ = azimuthal direction
$\perp$ = perpendicular to magnetic field

Presented at the AIAA Electric Propulsion Conference, Colorado Springs, Colo., March 11–13, 1963; revision received July 18, 1963. This work was sponsored by the Aeronautical Research Laboratories, Office of Aerospace Research, U. S. Air Force.

* Research Scientist, Electrical Propulsion Section, Research Laboratories.

† Associate Research Engineer, Electrical Propulsion Section, Research Laboratories.

‡ Chief, Electrical Propulsion Section, Research Laboratories.

Introduction

THE oscillating-electron ion engine[1,2] is a bombardment-type ion engine in which ions are generated and then electrostatically accelerated in an intense gaseous discharge. Although the geometry of this engine is simple (Fig. 1), the ion acceleration mechanism is quite complex, as it involves the establishment of axial electrostatic potential gradients in an essentially neutral plasma. Theoretical analyses as reported in Refs. 3 and 4 have shown that these potential gradients are supported by the reflection of trapped electrons having a nonthermal energy distribution. Some preliminary experiments had shown that these potential gradients were not present in the plasma under all operating conditions of the oscillating-electron discharge. Therefore, a more detailed investigation was undertaken to determine the effect of external operating parameters such as voltage, current, magnetic field strength, and mass flow on the behavior of the plasma within the engine. The results of this investigation which show the effects of these parameters on both steady-state and transient behavior of the plasma in the engine environment are reported herein.

Apparatus

Experiments with the oscillating-electron ion engine were performed in a 6-in.-diam Pyrex glass vacuum system that was connected to a 4-in. oil diffusion pump backed by a mechanical forepump. A schematic diagram of the vacuum envelope with the engine and external solenoids drawn to scale is shown in Fig. 2. Two sets of separately excited solenoids were used, the main solenoid and the downstream sole-

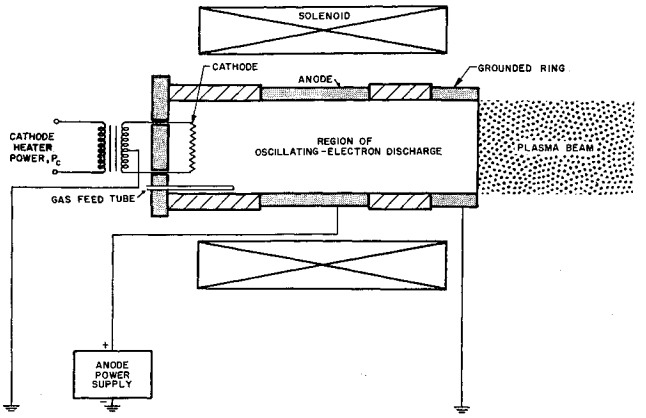

Fig. 1 Schematic diagram of oscillating-electron ion engine.

noid. By altering the ratio of downstream to main solenoid current, the magnetic field in the region between the engine and target could be varied from a divergent to a convergent configuration as shown in Fig. 2. The system was also provided with a movable target so that the plasma exhaust beam would be intercepted at different axial locations.

The cathode was a directly heated tantalum filament coated with lanthanum hexaboride. The other electrodes and the target were water-cooled and instrumented so that the power loss to the electrodes could be measured. Instantaneous currents and voltages associated with each electrode of the engine and the target were monitored with oscilloscopes. Both cold and hot Langmuir probes were used to measure electron densities, electron temperatures, and plasma potentials in both the engine and the exhaust beam. (The voltage-current characteristics of the probes were displayed on an oscilloscope.) These probes were located in the regions of the anode, grounded ring, and the exhaust beam. The anode and exhaust beam probes could be traversed radially across the plasma beam. Both the floating and plasma potentials were measured to within ± 5 v.

A continuous flow of gas was injected into the engine through a calibrated leak, and the mass flow was controlled by changing the pressure upstream of the leak. Pressure

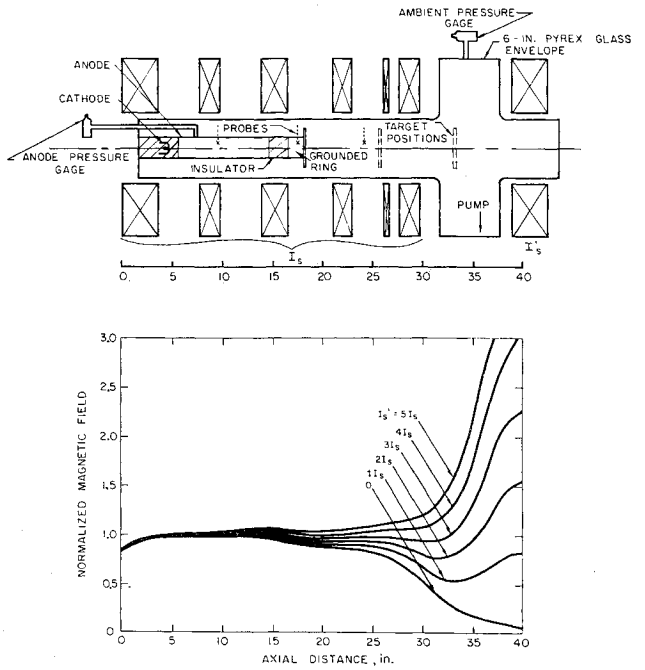

Fig. 2 Ion engine test configuration with variable downstream magnetic field.

measurements within the vacuum system were made using Veeco RG-75 ionization gages. Ambient pressure was monitored with a gage mounted on the top of the glass cross in the vicinity of the target; and anode pressure, the pressure inside of the engine, was monitored by means of a gage at the end of a Pyrex glass tubulation extended into the anode as shown in Fig. 2.

An electrostatic energy analyzer was mounted on the target to measure the energy distributions of the ions in the exhaust beam. Some ions passed through a pinhole in the target into the analyzer section. The operation of the analyzer involved passing this ion current through a decelerating field and collecting the transmitted current with a Faraday Cage collector. Only those ions which had energy greater than the potential drop across the retarding field could be collected. The ion energy distribution was obtained by determining the change of collector current with retarding potential. The geometry of the analyzer and a schematic of the associated electronic circuit are shown in Fig. 3. The first electrode was biased negatively to prevent electrons from reaching the collector; the second electrode was biased positively to create the retarding potential; and the third electrode was biased negatively to suppress secondary emission from the collector. The resolution of the analyzer was approximately ± 15 ev.

Results

Plasma Behavior within the Anode

The magnitude of the axial potential gradient within the engine was determined by measuring plasma potentials with probes located on the axis in the regions of the anode, grounded ring, and exhaust beam. In order to maintain the largest potential drop in the engine, it is essential that the plasma within the anode region be approximately equal to anode potential. Accordingly, the plasma within the anode was investigated in detail in order to ascertain the effect of engine operating conditions on the anode plasma potential. These measurements have also provided some insight into the mechanism of radial electron transport within the anode cavity. The charged particle densities observed during these tests ranged from 10^{10} to 10^{12}/cm^3, corresponding to a degree of ionization ranging from 0.1 to 10%.

The operating parameter that most strongly influenced the potential of the plasma within the anode cavity was the magnetic field. The most consistent sets of data illustrating the effect of magnetic field strength were obtained with operation at low anode current. Under this condition no axial potential gradients existed in the plasma, and the over-all operation was quiescent, i.e., no gross fluctuations of voltage or current occurred. The observed variation of anode plasma potential in an argon discharge of 200 v and 0.4 amp is shown

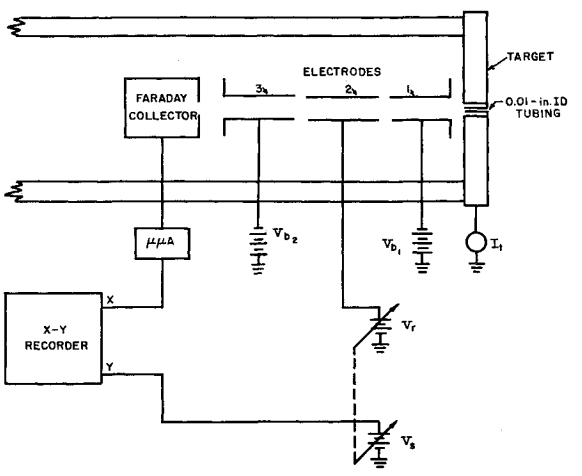

Fig. 3 Electrostatic ion energy analyzer.

in Fig. 4. Under this condition the plasma potential varied from 215 v at 300 gauss to 180 v for fields greater than 2000 gauss. These data represent the most extreme variation in anode plasma potential observed with argon. At higher pressures and/or lower currents the anode plasma potential deviated less from the applied anode voltage.

The variation of anode plasma potential with magnetic field is closely related to the diffusion rate of ions and electrons across the magnetic field. In the oscillating-electron ion engine, the current flow is determined ideally by the net flow of cathode electrons and target secondary electrons into the system and by the flow of ions out of the system, i.e., the particles that stream freely along magnetic field lines. However, in order to complete the electrical circuit, electrons must diffuse radially across magnetic field lines to reach the anode. An analysis by Simon[5] of a low-pressure plasma in the presence of an axial magnetic field, under the assumptions of no transverse electric field and free streaming of particles along field lines, yields an effective diffusion coefficient perpendicular to the magnetic field:

$$D_\perp \approx D_{i\perp} \approx \frac{D_i}{\omega_i^2 \tau_i^2} \sim \frac{T_i^{3/2} P_c p M_i^{1/2}}{B^2} \qquad (1)$$

where P_c is the probability of collision for the ions. The external parameters of anode voltage and current establish boundary conditions that must be satisfied by the plasma. If the diffusion of electrons does not provide the proper current flow to the anode, then the potential of the plasma will rise above that of the anode to inhibit electron flow or drop below that of the anode to enhance electron flow. In other words, radial electric fields are established which give rise to a mobility term contribution to the current flow.

The data presented in Fig. 4 indicate that at low magnetic fields the diffusion of electrons was more than sufficient to provide the proper current flow, but that as the magnetic field was increased the diffusion coefficient decreased until finally the plasma potential assumed a value lower than that of the anode. At the higher magnetic fields, electron transport due to the radial electric field augmented the radial diffusion and the plasma "detached" from the anode. Similar results were obtained with neon and krypton. It might be expected that detachment would occur more readily with lighter gases because of the lower diffusion coefficient as indicated by Eq. (1). This hypothesis was verified by the results obtained with hydrogen gas shown in Fig. 5. The mass and collision probability of hydrogen are significantly different from either argon or neon, so that the effect should be more pronounced even if densities and temperatures were

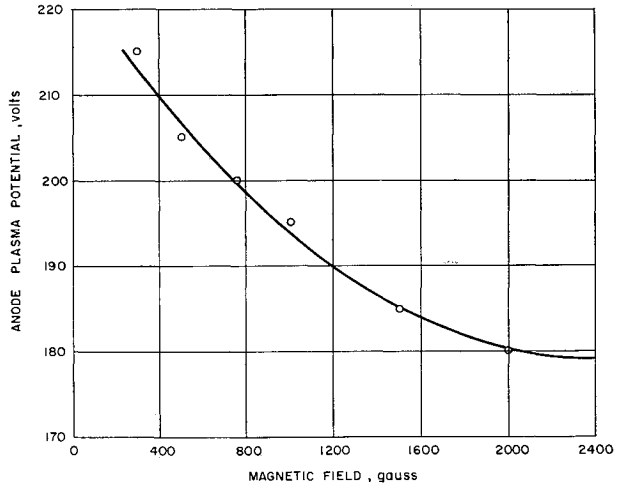

Fig. 4 Anode plasma potential variation. Operating conditions: argon; $p_{amb} = 1 \times 10^{-4}$ mm Hg; $V_a = 200$ v; $I_a = 0.4$ amp.

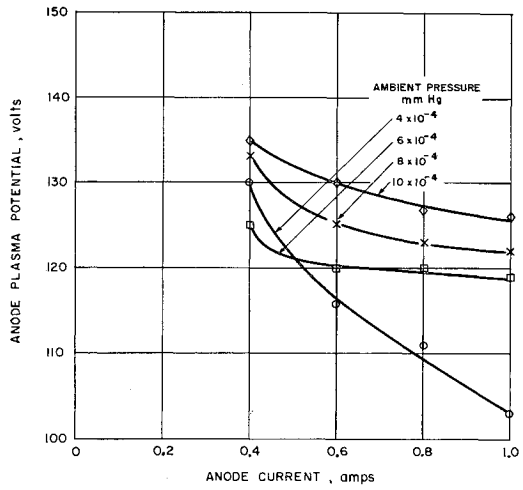

Fig. 5 Anode plasma potential variation. Operating conditions: hydrogen; $V_a = 200$ v; $B = 500$ gauss.

slightly different. For a magnetic field of only 500 gauss, the anode plasma potential was less than 140 v with an applied anode potential of 200 v. The data in Fig. 5 also show that the anode plasma potential decreased slightly with decreasing pressure and with increasing current. Both of these variations would be expected if the charge particle density and electron and ion temperatures remained constant.

For sufficiently strong magnetic fields, other experimenters[6] have observed that the entire discharge voltage drop is distributed radially. However, in the oscillating-electron ion engine under typical operating conditions with argon or krypton, the plasma potential within the anode was always observed to be close to the applied anode potential, so that the plasma potential variations were predominantly in the axial direction.

Plasma Potential Gradients

The existence of axial potential gradients in the plasma within the oscillating-electron ion engine have been reported previously in Refs. 1–3. In the investigations described herein, potential distributions were not determined in detail. Instead, the effect of several independent variables on the over-all axial potential drop were determined. The axial plasma potential drop was measured by means of three probes; these were located in the regions of the anode, grounded ring, and exhaust beam, as shown in Fig. 2. Furthermore, since most of the experiments were performed with argon, the potential of the plasma within the anode was always within ± 20 v of anode potential. It was also found that the potentials measured by the grounded ring and exhaust beam probes were generally in agreement within experimental accuracy. Hence the full potential drop occurred in the region between the anode and grounded ring.

Effect of anode current and voltage

With magnetic field strength, anode voltage, and gas pressure held constant it was necessary to increase the anode current (by increasing the cathode emission level) above some critical value in order to achieve an axial potential drop in the plasma. As seen in Fig. 6, the anode plasma potential was equal to or slightly greater than the applied potential for all anode currents. Both the exhaust beam and ground ring plasma potential were equal to anode potential at the lower anode currents. At these lower currents, the full potential drop from anode to ground potential occurred in sheaths at the cathode, ground ring, and target. However, as the anode current was increased above 0.8 amp, a potential drop appeared in the plasma as evidenced by the lowering of both

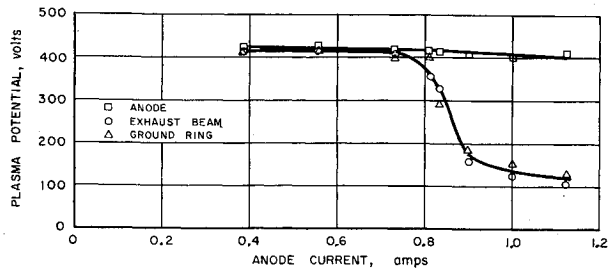

Fig. 6 Effect of anode current on plasma potentials. Operating conditions: argon; $p_a = 5.2 \times 10^{-4}$ mm Hg; $p_{amb} = 6.8 \times 10^{-5}$ mm Hg; $V_a = 400$ v; $B = 550$ gauss.

the exhaust beam and ground ring plasma potentials, which were approximately equal. As the current was further increased, the potential drop increased until a minimum exhaust beam potential of approximately 100 v was reached. As will be discussed in a subsequent section, this minimum potential was considerably above ground potential because of a relatively high ambient pressure in the test system.

The anode current required to achieve a potential drop in the plasma was essentially independent of the applied anode voltage, as shown in Fig. 7. However, higher relative potential drops were achieved with higher applied voltages. The solid data points in Fig. 7 were obtained while the engine was in a fluctuating or unsteady mode of operation. This unsteady operation occurred when the current was increased slightly above that required to achieve the minimum exhaust beam potential. This fluctuating mode of operation is described in some detail in a later section.

Effect of pressure

The mass flow ($\dot{m}$) of gas into the engine and the anode and ambient pressure (p_a and p_{amb}, respectively) could not all be controlled independently in these experiments. However, different combinations of these variables were obtained by changing the mass flow and by throttling the vacuum system pumping speed (by means of a valve between the diffusion pump and the test section). For the most part it was desirable to maintain the ambient pressure in the system as low as possible in order best to simulate a space environment. Therefore, most of the tests were performed with the throttling valve wide open. Under this condition p_{amb} was about one order of magnitude lower than p_a over the range of mass flow used in the experiments.

The axial potential gradients in the plasma were found to be quite strongly dependent on the anode pressure. The general variation of plasma potential with anode current was similar to that shown in Fig. 6 for all operating pressures. However, as the anode pressure was increased, a higher anode current was required to achieve an equivalent potential drop in the plasma. This dependence on pressure is clearly illustrated in Fig. 8, where the anode current required to lower the exhaust beam potential V_{pE} from 400 to 200 v is observed

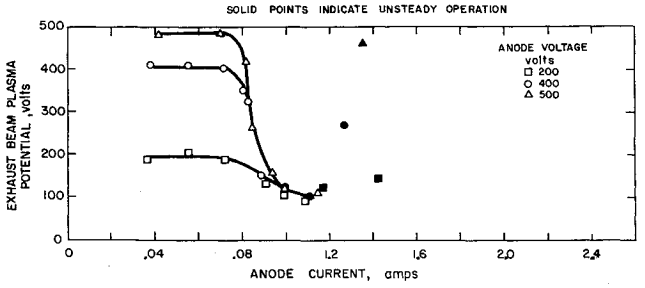

Fig. 7 Effect of anode voltage on plasma potentials. Operating conditions: argon; $p_a = 5.2 \times 10^{-4}$ mm Hg; $p_{amb} = 6.5 \times 10^{-5}$ mm Hg; $B = 550$ gauss.

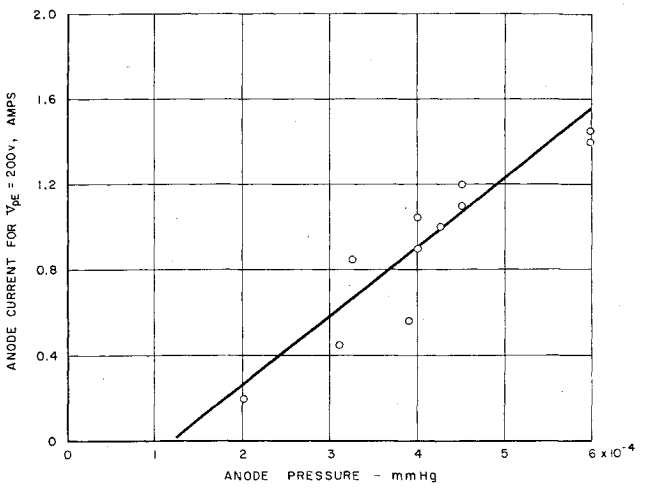

Fig. 8 Effect of anode pressure on plasma potential-anode current dependence. Operating conditions: argon; $V_a = 400$ v; $B = 275$ gauss.

to increase with increasing anode pressure. Although there is considerable scatter in the data, to a first approximation the anode current increases linearly with anode pressure over the range of pressures investigated.

The existence of a high ambient pressure in the system had an adverse effect on the formation of axial potential gradients in the plasma. With the anode pressure held constant, higher anode currents were required to maintain a gradient in the plasma as the ambient pressure was increased. More generally, any change that resulted in the creation of more ion-electron pairs downstream of the electrodes had an adverse effect on the formation of the potential gradient. For example, when the target was moved further downstream from the engine, more ion-electron pairs were formed outside of the engine, and, consequently, higher currents were required to maintain the gradient in the plasma. On the other hand, with smaller diameter engines, in which higher ratios of p_a to p_{amb} could be obtained for a given mass flow, lower anode currents were required to maintain a gradient in the plasma. The adverse effect of ion-electron pairs created outside of the engine is consistent with the theory of space-charge neutral ion acceleration as discussed in Refs. 3 and 4. Collisions, especially ionizing collisions, that occur outside of the engine result in an increased number of electrons that are ultimately accelerated back into the engine. In order to preserve charge neutrality, the exhaust beam plasma potential increases to inhibit the flow of ions from the engine. Thus, the potential drop decreases.

The creation of a large number of ion-electron pairs downstream of the engine electrodes is clearly illustrated in Figs. 9 and 10. In Fig. 9 the characteristic variation of exhaust beam potential with anode current is shown for a typical operating condition. Ion energy distributions (obtained with the ion energy analyzer shown in Fig. 3) associated with each data point in Fig. 9 are presented in Fig. 10. The energy in electron volts corresponding to the peaks of the distributions in Fig. 10 are also plotted in Fig. 9 for convenient comparison. At low anode currents, with no axial potential gradient, all of the ions which entered the analyzer were accelerated through the full applied voltage in a sheath at the target. However, with an axial potential gradient in the plasma, there were two distinct energy groups of ions in the distributions, one centered around the exhaust beam potential, and one close to anode potential. The relative intensities of the two groups indicate that the ions created outside of the engine should have had a highly adverse effect on the performance of the engine. Thus, the evaluation of ion engine performance from results of experiments in this relatively small vacuum system is not feasible, indicating the need for tests in a large vacuum chamber such as the one reported in Ref. 7.

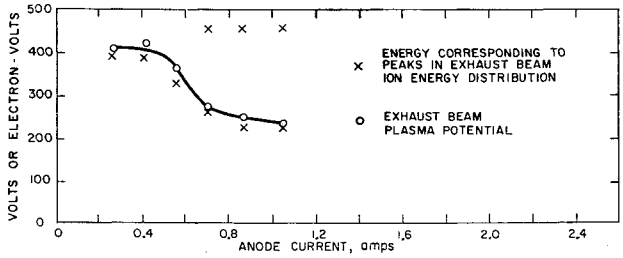

Fig. 9 Characteristic exhaust beam potentials. Operating conditions: argon; $p_a = 3.8 \times 10^{-4}$ mm Hg; $p_{amb} = 3.5 \times 10^{-5}$ mm Hg; $V_a = 400$ v; $B = 275$ gauss.

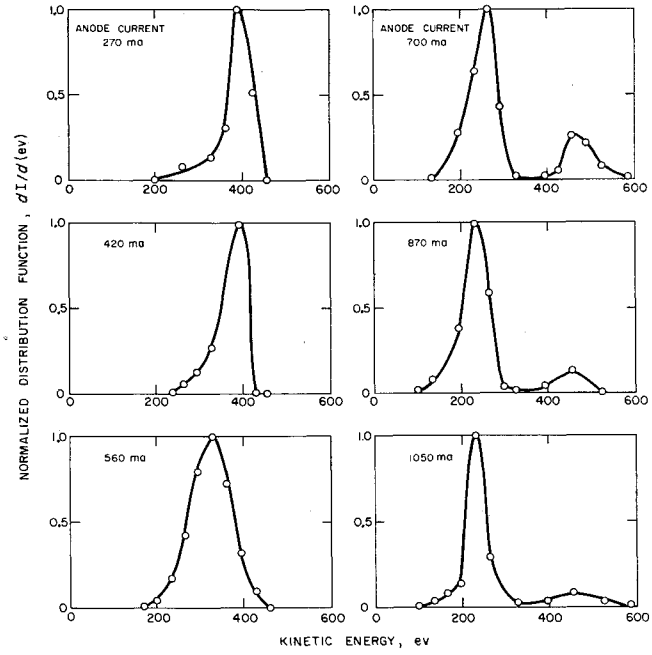

Fig. 10 Exhaust beam ion energy distributions at operating points shown in Fig. 9.

Effect of magnetic field

The majority of experiments with the ion engine were carried out in a magnetic field that was uniform throughout the whole discharge region, i.e., from the cathode to the target. For a fixed operating pressure, it was found that potential gradients could be maintained in the plasma with lower anode currents as the strength of the magnetic field was increased. This dependence on magnetic field strength is illustrated in Fig. 11, in which the anode current required to lower the exhaust beam potential V_{pE} to 200 v (out of 400 v applied) is seen to decrease approximately as $1/B$. This type of dependence on magnetic field was observed throughout the range of operating pressures employed. The indication is that, within certain limits, higher magnetic fields should result in higher engine efficiencies.

As described previously and shown in Fig. 2, the divergence of the magnetic field in the region between the engine and the target could be varied by changing the ratio of the current in the downstream solenoid (I_s') to that in the main solenoid (I_s). With $I_s' = 3I_s$, the field was uniform to within 5%. For higher values of I_s' the field was convergent toward the target, and for lower values, i.e., less than $3I_s$, the field was divergent. It should be noted that most of the change in the field occurred outside of the engine. However, changing the divergence of the field in this region had a very pronounced effect on the formation of potential gradients in the plasma. As shown in Fig. 12, as the field was made more divergent the exhaust beam potential decreased, and as the field was made convergent the exhaust beam potential increased. The reason for this effect of magnetic field divergence is that the

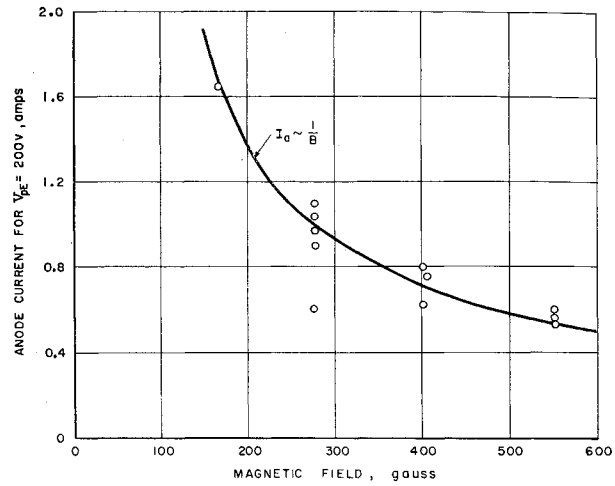

Fig. 11 Effect of magnetic field on plasma potential-anode current dependence. Operating conditions: argon; $p_a = 4.0 \times 10^{-4}$ mm Hg; $p_{amb} = 5.2 \times 10^{-5}$ mm Hg; $V_a = 400$ v.

diverging field tends to nullify the adverse effect of high ambient pressure. With a diverging field, electrons formed by ionizations outside of the engine tend to be reflected by the magnetic field instead of being accelerated back into the engine. Hence, certain electrons (i.e., those with a sufficiently high transverse velocity) are blocked from the engine and cannot contribute to a charge density imbalance, which, as has been discussed previously, would tend to reduce the axial potential drop. This effect is also quite significant because it indicates that magnetic field divergence should have a beneficial effect on engine performance. Of course, any ion engine operating in space would necessarily have a divergent field because of the finite length of the engine solenoid. The test results presented in Fig. 12 indicate that this divergence could be used to advantage in improving the efficiency of the engine.

Instabilities

Plasma oscillations

In experiments with a discharge somewhat similar to that within the oscillating-electron ion engine, Bingham et al.[8] have reported rotation of the plasma at a frequency corresponding to an azimuthal drift velocity of $\mathbf{E}_r \times \mathbf{B}_x/B^2$, where E_r is the radial electric field and B_x is the axial magnetic field. In order to determine whether or not similar effects occurred within the oscillating-electron engine, three additional probes were installed in the anode cavity in a plane normal to the axis, as shown in the top of Fig. 13. These probes were located 90° and 180° apart azimuthally, with the sensitive areas $\frac{3}{8}$ in. from the anode wall. Experiments were performed with the outputs of two of the probes displayed on the two channels of a dual-beam oscilloscope. The signals monitored were the floating potentials of the probes. With a 9-kc high-pass filter inserted in the output circuit of each probe,

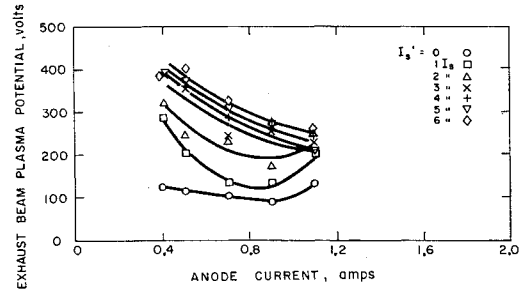

Fig. 12 Effect of magnetic field divergence on plasma potentials (magnetic field distributions shown in Fig. 2). Operating conditions: argon; $p_a = 4.1 \times 10^{-4}$ mm Hg; $p_{amb} = 5.6 \times 10^{-5}$ mm Hg; $V_a = 400$ v; $B = 275$ gauss.

coherent signals in the range of 15 to 50 kc were observed. Furthermore, phase shifts in the probe signals indicated that the plasma or some plasma perturbation was rotating. Waveforms obtained at two different frequencies are shown in Fig. 13. The staging of the probes was such that, viewed from the cathode end of the engine, probes 1, 2, and 3 were in clockwise rotation, each 90° apart. As shown in Fig. 13, the signals at probes 2 and 3 were out of phase by approximately 90°, indicating rotation. Furthermore, it was found that the direction of rotation could be reversed by reversing the direction of the applied magnetic field. This result is consistent with the hypothesis that the rotation of the plasma is due to an azimuthal drift corresponding to $\mathbf{E}_r \times \mathbf{B}_x/B^2$.

To investigate further the nature of the observed rotation, the strength of the magnetic field was varied while the mass flow and/or pressure and the anode current and voltage were kept constant. Tests were conducted at several different currents, voltages, and mass flows. The results of these tests are presented in Fig. 14 and show that the rotational frequency was only weakly dependent on pressure, anode current, and anode voltage but was strongly dependent on the magnetic field up to a field strength of 500 gauss. For the range of magnetic field employed, the observed frequencies would require an electric field on the order of 1 v/cm. The solid curve in Fig. 14 represents the theoretical rotational frequency for a radial electric field E_r of 1.25 v/cm and a radius of 2 cm. This value of electric field is well within the accuracy of measurements of E_r with Langmuir probes.

One of the most significant consequences of this investigation was the observation that the direction of rotation reversed as the magnetic field strength was increased. This reversal occurred at a magnetic field strength of approximately 500 gauss. At lower magnetic fields the rotation was counterclockwise, indicating that, if the rotation was associated with an $\mathbf{E}_r \times \mathbf{B}_x$ drift, E_r was directed radially outward, whereas at higher magnetic fields the rotation was clockwise, indicating that E_r was directed radially inward. This reversal in rotation is illustrated in the two oscillograms presented in Fig. 13. The corresponding reversal of E_r is consistent with results of the anode plasma potential measurements. It was noted that the potential of the plasma in the anode region varied from a value greater than anode potential to a value less than anode potential as the magnetic field strength was increased. However, the critical magnetic field for reversal was more difficult to determine accurately from probe measurements because these measurements were accurate to only

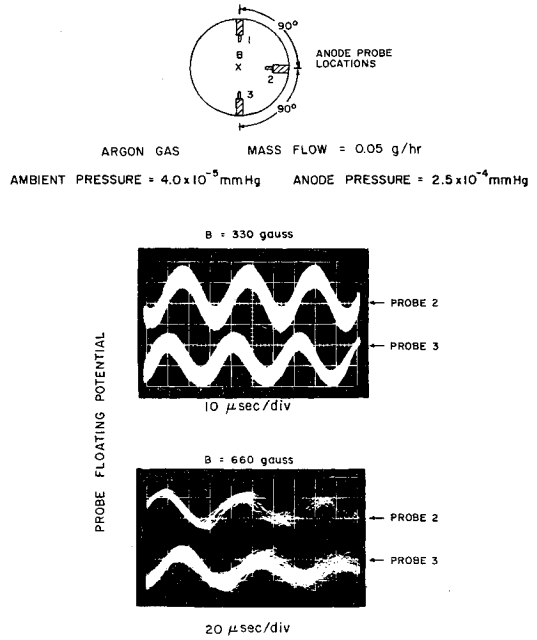

Fig. 13 Plasma oscillations.

SYMBOL	MASS FLOW g/hr	ANODE PRESSURE mm Hg	AMBIENT PRESSURE mm Hg	ANODE VOLTAGE volts	ANODE CURRENT amps
○	0.075	4.6×10^{-4}	5.7×10^{-5}	400	0.20
△	0.075	4.6×10^{-4}	5.7×10^{-5}	400	0.33
□	0.075	4.6×10^{-4}	5.7×10^{-5}	400	0.50
×	0.125	$\approx 7.0 \times 10^{-4}$	8.5×10^{-5}	400	0.50
◇	0.125	$\approx 7.0 \times 10^{-4}$	8.5×10^{-5}	200	0.50

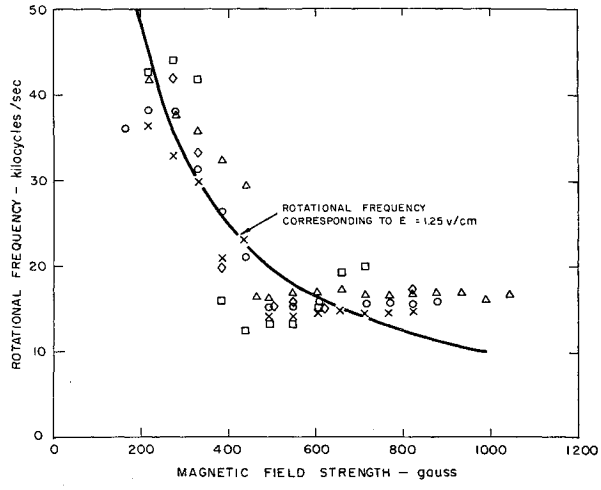

Fig. 14 Effect of magnetic field on plasma rotational frequency; operation with argon.

±5 v. The results of the plasma potential measurements are in agreement with the results of the rotation measurements within this accuracy.

At present the nature of the observed plasma rotation is not completely understood. For example, it has not been determined whether the rotating perturbations are sustained indefinitely or whether they are local perturbations with relaxation or decay times lasting for several periods of rotation. Signals observed at probes located at the same azimuthal station, but spaced 10 cm apart axially, were found to be in synchronism. However, because charged particles can stream freely along field lines, even "local" perturbations have axial characteristic lengths comparable to the length of the discharge. The rotational character of the perturbations suggest the possibility that these oscillations may be related to a plasma screw instability, which was first described for high pressure discharges by Kadomtsev[9] and later by Guest and Simon[10] for low-pressure discharges. The waveforms shown in Fig. 13 are similar to those observed in a high-pressure discharge with the presence of a screw instability as reported by Paulikas and Pyle in Ref. 11. In the present low-pressure discharge, the wavelength of such a helical disturbance would be considerably larger than the axial dimensions of the engine. Thus, no axial phase shift would be expected, and it would not be possible to detect the presence of a screw instability. In addition, no critical field for onset of the oscillations was observed. Hence, it has not been definitely established whether or not the rotations are, in fact, due to a screw instability. At present, however, it is felt that, even if the rotation is not related to a screw instability, it could contribute to enhanced diffusion by a similar mechanism. Such enhanced diffusion would occur if the entire plasma rotated as a result of an $\mathbf{E}_r \times \mathbf{B}_x$ drift. Any azimuthal perturbation in the plasma density, for example, would result in the formation of an azimuthal electric field E_θ due to differences in ion and electron drift velocities resulting from collisions with neutrals. Drifts due to the presence of E_θ would occur in the radial (i.e., the $\mathbf{E}_\theta \times \mathbf{B}_x$) direction in a manner similar to drifts in the Kadomtsev theory.

Fluctuations

Under certain conditions, the engine exhibited a cyclic on-off type of operation. For a constant operating pressure, mag-

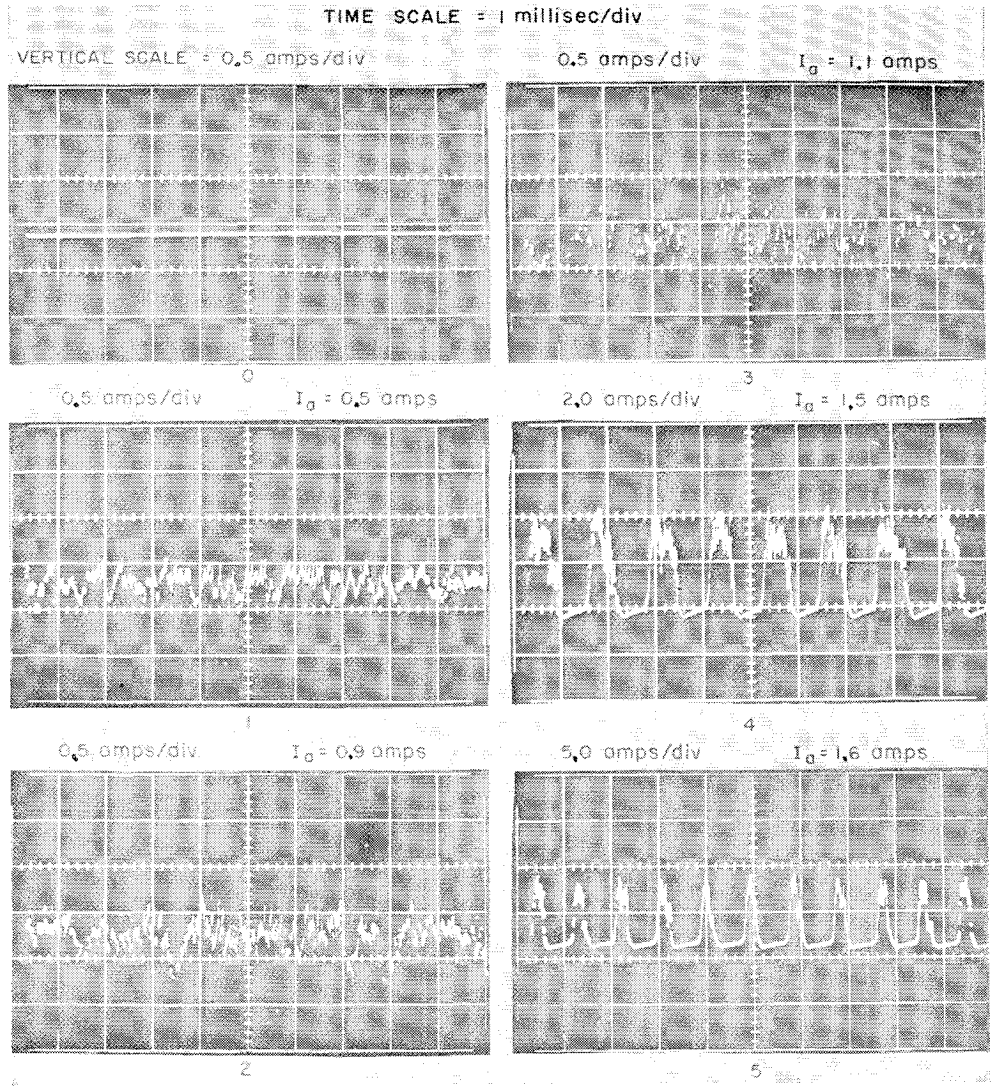

Fig. 15 Anode current waveforms. Operating conditions: argon; $p_{amb} = 1.0 \times 10^{-4}$ mm Hg; $V_a = 400$ v; $B = 1500$ gauss.

netic field, and anode voltage, the onset of this unsteady operation occurred when the anode current, as controlled by the cathode emission level, exceeded some critical value $I_{a\,crit}$. This transition is illustrated in the set of oscillograph records of anode current waveforms, which are presented in Fig. 15. The anode currents I_a recorded in the figure are the d.c. or time-average currents as determined from d.c. meters. At low anode currents, the waveforms show the presence of incoherent noise. However, at some current between 1.1 and 1.5 amp, the waveforms become coherent and, at all higher currents, exhibit a cyclic variation as shown in the last two oscillograms in Fig. 15. Careful examination of the current waveforms and the light output of the engine (by means of a phototube) show that the engine operated for a short time and then shut off completely. These fluctuations were characteristic of over-all engine operation and were observed in synchronism at all electrodes.

The value of I_a at which the fluctuations appeared was found to be independent of anode voltage but dependent on magnetic field strength and pressure. The variation of $I_{a\,crit}$ with mass flow and the corresponding initial anode pressure (i.e., the pressure measured with $I_a = 0$) is shown in Fig. 16. For operation at each of the values of magnetic field strength, $I_{a\,crit}$ increased with increasing mass flow. For a given mass flow, the value of $I_{a\,crit}$ decreased as the magnetic field strength was increased, as shown in Fig. 17. From these data it is seen that for low magnetic fields (less than 1000 gauss) $I_{a\,crit}$ varies with anode pressure and magnetic field strength approximately as p_a/B.

An explanation of the cause of the fluctuations, which is in agreement with the observed performance, is that the production and acceleration of ions out of the engine is an effective pumping mechanism that reduces anode pressure to the point at which the discharge is extinguished. During the off-time, the gas is replenished until the pressure reaches a value that permits the initiation of a discharge. This effect of pressure has been noted in previous experiments in which it was observed that a discharge could not be sustained in the engine below a certain critical pressure, and that this critical value increased as magnetic field strength increased. As shown earlier, it is necessary that the anode current be above a certain value in order for potential gradients to be maintained within the plasma. This is in agreement with the data (Fig. 15) showing that the anode current must increase to a certain critical value in order for fluctuations to occur. This critical value of anode current is above the value of anode current at which potential gradients are first observed. The dependence of $I_{a\,crit}$ on magnetic field strength (Fig. 17) is consistent with this theory, since larger gradients (hence greater pumping action) and higher minimum pressure for discharge operation are associated with higher magnetic fields.

Detailed examination of the anode current waveforms yielded results in agreement with the pumping theory. In the fluctuating mode of operation, an increase in average anode current resulted in larger anode current peaks, but for a given mass flow the off-time of the discharge remained approximately constant. The fact that the mass flow controlled the off-time was further verified experimentally. The mass flow was varied, and the ambient pressure was held constant by throttling the pumping speed of the system. The off-time

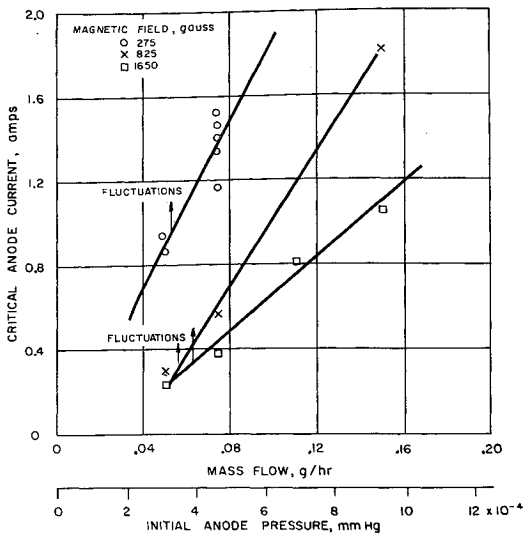

Fig. 16 Effect of mass flow on critical anode current for fluctuations. Operating conditions: argon; V_a = 400 v.

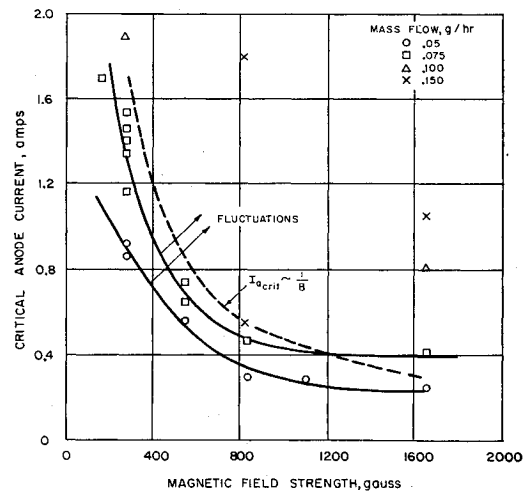

Fig. 17 Effect of magnetic field on critical anode current for fluctuations. Operating conditions: argon; V_a = 400 v.

under these conditions decreased linearly with increasing mass flow. Calculation of the fill-up time of the engine, assuming a pressure drop of a factor of 2 during fluctuating operation, gave values of the same order of magnitude as the measured values of the off-time of the discharge.

Attempts to measure the variation of anode pressure with time, using a gage attached to the anode, were unsuccessful because of interference by the plasma. A time-averaged measurement of the anode pressure, as monitored with an ion gage on the tube extending from the anode electrode, showed that the pressure decreased with increasing anode current. Although direct measurements of the time variation of the anode pressure could not be made, all of the experimental results obtained to date are consistent with the theory that pumping action is the cause of these fluctuations within the engine.

Conclusion

The important results and conclusions from this investigation are as follows:

1) The potential of the plasma in the anode region of the oscillating-electron ion engine is controlled by charged particle transport properties across the magnetic field. In the usual operating regime of the engine, this potential is approximately equal to the applied anode potential, except in discharges employing very light gases such as hydrogen and possibly helium.

2) Axial electrostatic potential gradients can be maintained in the neutral plasma within the engine by operating the engine at a sufficiently high anode current level. The required anode current level varies directly with anode pressure and inversely with magnetic field strength and is independent of the applied anode voltage.

3) The production of ion-electron pairs outside of the engine tends to destroy the axial potential gradient in the plasma. For a meaningful evaluation of ion engine performance, this effect must be minimized by maintaining the ambient pressure at least two orders of magnitude lower than the gas pressure inside of the engine.

4) The effect of a diverging magnetic field in the region of the plasma exhaust beam (as would be the case for an engine employing a solenoid of finite length) is to enhance the axial potential drop. Thus, from this standpoint, the finite length of an engine solenoid should be beneficial to performance.

5) A rotation of the plasma or plasma perturbation can occur within the engine and appears to be due to an $\mathbf{E}_r \times \mathbf{B}_x/B^2$ drift. It has been postulated that this drift may result in an enhanced loss of electrons from the discharge by a mechanism similar to that of a plasma screw instability.

6) Under conditions of high anode current, the oscillating-electron ion engine exhibits a fluctuating, or repetitive, on-off type of operation. This fluctuating mode appears to be caused by the pumping action of the discharge which decreases the gas pressure below a critical value for maintaining the discharge.

Since the completion of the experiments reported in this paper, oscillating-electron ion engines have been tested in a large vacuum facility. The results of these latter tests, reported in Ref. 7, are in general agreement with those presented in this paper. More specifically, the functional dependences of the plasma properties on the operating parameters are in agreement in both cases, whereas the actual current levels differ because of large differences in mass flow and pressure in the two systems.

References

[1] Meyerand, R. G., Jr., "The oscillating-electron plasma source," *ARS Progress in Astronautics and Rocketry: Electrostatic Propulsion* (Academic Press, New York, 1961), Vol. 5, pp. 81–90.

[2] Davis, J. W., Walch, A. P., Meyerand, R. G., Jr., Salz, F., and Lary, E. C., "Theoretical and experimental description of the oscillating-electron ion engine," IAS-ARS Preprint 61-103-1797 (1961).

[3] Salz, F., Meyerand, R. G., Jr., Lary, E. C., and Walch, A. P., "Electrostatic potential gradients in a Penning discharge," Phys. Rev. Letters **6**, 523–525 (1961).

[4] Davis, J. W., Angelbeck, A. W., and Pinsley, E. A., "Research on the oscillating-electron plasma source," Aeronaut. Res. Labs. Rept. ARL62-471, Contract AF 33(616)-7448 (1962).

[5] Simon, A., "Diffusion of arc plasmas across a magnetic field," Proc. 2nd Intern. Conf. Peaceful Uses of Atomic Energy (Geneva) **32**, 343–348 (1958).

[6] Chen, F. F., "Radial electric field in a reflex discharge," Phys. Rev. Letters **8**, 234–237 (1962).

[7] Pinsley, E. A., Walch, A. P., Churchill, T. L., and Banas, C. M., "Investigation of the oscillating-electron ion engine for space application," United Aircraft Corp. Res. Labs. Rept. A910002-1 on Contract AF 33(616)-8376, ASD-TDR-62-410 (1962); confidential.

[8] Bingham, R. L., Chen, F. F., and Harries, W. L., "Preliminary studies of a reflex arc," Princeton Univ., Plasma Phys. Lab. Rept. MATT-63 (1962).

[9] Kadomtsev, B. B. and Nedospasov, A. V., "Instability of the positive column in a magnetic field and the 'anomalous' diffusion effect," J. Nuclear Energy **1C**, 230–235 (1960).

[10] Guest, G. and Simon, A., "Instability in low-pressure diffusion experiments," Phys. Fluids **5**, 503–509 (1962).

[11] Paulikas, G. A. and Pyle, R. V., "Macroscopic instability of the positive column in a magnetic field," Phys. Fluids **5**, 348–360 (1962).